Chemical Geology 493 (2018) 100–108

Contents lists available at ScienceDirect

Chemical Geology

journal homepage: www.elsevier.com/locate/chemgeo

High-precision analysis of potassium isotopes by HR-MC-ICPMS

Yan Hu[a,*], Xin-Yang Chen[a], Ying-Kui Xu[a,b], Fang-Zhen Teng[a,*]

[a] Isotope Laboratory, Department of Earth and Space Sciences, University of Washington, Seattle, WA 98195-1310, USA
[b] Lunar and Planetary Science Research Center, Institute of Geochemistry, Chinese Academy of Sciences, Guiyang, Guizhou 550081, China

ARTICLE INFO

Editor: Catherine Chauvel

Keywords:
K isotopes
HR-MC-ICPMS
High-precision
Cold plasma
Dry plasma

ABSTRACT

This study presents a method for high-precision stable potassium (K) isotope analysis using High-Resolution Multi-Collector Inductively Coupled Plasma Mass Spectrometry (HR-MC-ICPMS). Dry and cold plasma is used to suppress the formation of argon hydrides that are direct isobaric interferences on K isotopes. The residual $^{40}Ar^{1}H^{+}$ beam is resolved from $^{41}K^{+}$ by using pseudo-high resolution mode, providing interference-free shoulders of $^{39}K^{+}$ and $^{41}K^{+}$ for isotopic measurements. Precision of better than 0.06‰ (95% confidence interval) has been routinely achieved based on multiple measurements of pure K standard solutions and rock standards over a six-month period. Mismatches in K concentration (up to 20%) and acid molarity (up to 67%) between samples and bracketing standards, as well as the presence of substantial amount of matrix element Rb, do not significantly affect the analytical precision and accuracy. Our study documents that high-precision K isotope analysis can be routinely achieved for a wide variety of natural samples by HR-MC-ICPMS, which makes it possible for using K isotopes to trace major geological processes.

1. Introduction

Potassium (K) is a moderately volatile, fluid-mobile, and lithophile element concentrated in the crust and ocean, and is an essential metabolic element for both animals and plants (Arevalo, 2016). The relatively large mass difference (5%) between the two stable K isotopes (^{41}K, 6.730% and ^{39}K, 93.258%; Berglund and Wieser, 2011) indicates that potentially large mass-dependent fractionation may occur in a variety of chemical and biological processes, which has motivated exploration of K isotopic variation since 1930s (e.g., Brewer, 1936, 1937; Nier, 1936, 1950; Taylor and Urey, 1938). However, the application of K isotopes has mostly been limited to biological/nutritional investigation on K cycling and evaporation/condensation-related planetary processes because these processes produce large isotope fractionations (up to 183‰, Taylor et al., 2005) that could be distinguished with relatively low analytical precisions, e.g., 3‰ to 10‰ by single collector ICP-MS (Jiang et al., 1988; Becker and Dietze, 1998; Murphy et al., 2002; Becker et al., 2008), ≥1.0‰ by thermal ionization mass spectrometry (TIMS) (Barnes et al., 1973; Garner et al., 1975; Church et al., 1976; Gramlich et al., 1982; Midwood et al., 2000), and ≥0.5‰ by secondary ionization mass spectrometry (SIMS) (Humayun and Clayton, 1995a, 1995b; Alexander et al., 2000; Yu et al., 2003; Humayun and Koeberl, 2004; Alexander and Grossman, 2005).

The advent of MC-ICPMS has made it possible to measure K isotopes with higher precision (internal precision < 0.1‰; Wang and Jacobsen, 2016; Li et al., 2016; Morgan et al., 2018). The main challenge, however, is to avoid the intense interference from $^{40}Ar^{+}$ and argon hydrides ($^{38}Ar^{1}H^{+}$ and $^{40}Ar^{1}H^{+}$) produced in the Ar plasma. Two strategies have been used to eliminate this analytical barrier. Richter et al. (2011, 2014), Li et al. (2016), and Wang and Jacobsen (2016) used the collision cell on IsoProbe-P MC-ICPMS to remove Ar-based ionic species. Potassium isotopes can then be measured in low resolution mode, achieving a typical external precision (2SD) of 0.20‰ to 0.30‰. However, the use of a collision cell requires an additional cost for high-purity reaction gases and is also hindered by its inability to be an upgrade to existing instruments.

The alternative approach to suppress Ar-based interference is to use cold plasma by reducing the radio frequency (RF) forward power because Ar has a much higher ionization energy of 15.76 eV than K (4.34 eV) (Jiang et al., 1988). The residual interference of Ar hydrides can then be partially separated by using high mass resolution (Fig. 1). This technique has recently been applied on a Neptune Plus MC-ICPMS with a claimed external precision of 0.17‰ (2SD) (Morgan et al., 2018). However, since δ^{41}K values of chemically-purified seawater vary by 0.49‰ between different analytical sessions, they have to normalize each batch of the measured sample δ^{41}K values to that of the seawater analyzed in the same session to reach an improved external reproducibility of 0.02‰ to 0.34‰ (2SD) (Morgan et al., 2018). This additional correction step may introduce unwanted uncertainty to their results, particularly given that the 81 natural samples investigated in that study

* Corresponding authors.
E-mail addresses: yanhu@uw.edu (Y. Hu), fteng@uw.edu (F.-Z. Teng).

https://doi.org/10.1016/j.chemgeo.2018.05.033
Received 6 January 2018; Received in revised form 14 May 2018; Accepted 22 May 2018
Available online 24 May 2018

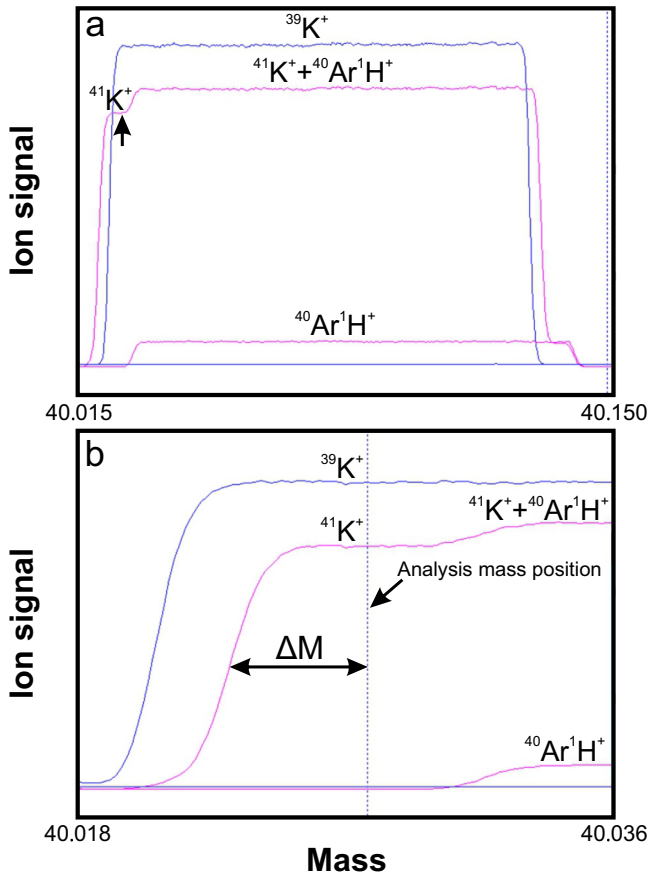

Fig. 1. Integration of 5 peak scans for masses 39 and 41 at 500-step resolution (a) and 100-step resolution (b) performed on a Nu Plasma II MC-ICPMS displaying K isotopes and associated argon hydride interference. Since $^{41}K^+$ has a slightly lower mass than $^{40}Ar^1H^+$, it appears first in a scan and forms an interference-free peak shoulder. The black arrow in (a) emphasizes the narrow $^{41}K^+$ peak shoulder. Analysis mass position is determined by the selected ΔM value, which is the measured offset from the position at half height of the peak shoulder. (Beam intensities for $^{39}K^+$ = 6.55 V, $^{41}K^+$ = 0.515 V, $^{40}Ar^1H^+$ = 0.05 V; therefore, $^{40}Ar^1H^+/^{41}K^+$ = 0.1).

were only measured twice on average. Considering the relatively small terrestrial variation in $\delta^{41}K$, the accuracy and precision of K isotope measurements using cold plasma in high resolution mode merits further evaluation and that is the focus of this study.

In this paper, we tailored an analytical protocol for K isotope measurements on a Nu Plasma II MC-ICPMS by using a reduced RF forward power in high-resolution mode with a DSN-100 desolvation nebulizer system (i.e., "dry" plasma). Our results demonstrate that high-precision K isotopic analysis (better than 0.06‰, 95% confidence interval, c.i.) can be routinely achieved for diverse geological samples. This study indicates the potential for using K isotopes to trace geological and biological processes that have sub-permil variations in $\delta^{41}K$.

2. Analytical methodology

All the experimental and analytical work in this study was conducted in the Isotope Laboratory at the University of Washington, Seattle. Sample dissolution and column chemistry were done in class 100 vented laminar flow hoods in a class 10,000 clean laboratory.

2.1. Reagents, materials, and standards

Milli-Q water, distilled ultrapure acids and Teflon beakers were used exclusively in this study. Six international rock standards from United States Geological Survey (USGS) were processed and analyzed to assess the accuracy and whole-procedure reproducibility. The standards were selected to represent a full spectrum of possible matrix types, including basalt (BHVO-1 and BCR-1), andesite (AGV-1), granodiorite (GSP-1), granite (G-2), as well as a sedimentary standard (SGR-1). These standards have been used in other laboratories that study K isotopes and thus permit inter-laboratory comparisons (Humayun and Clayton, 1995b; Wang and Jacobsen, 2016; Li et al., 2016; Morgan et al., 2018).

2.2. Sample digestion and chemical separation of K

Powdered rock standards were dissolved by successive additions of Optima grade (Fisher Scientific) concentrated HF-HNO_3 mixture, HCl-HNO_3 mixture, and HNO_3. The digested sample solutions were evaporated to dryness after each step of acid addition. The shale standard SGR-1 was treated in addition with Optima grade H_2O_2 to oxidize the organics. An aliquot of Hawaiian seawater was evaporated to dryness and then redissolved in concentrated HNO_3. Following complete digestion, all samples were redissolved in 0.5 N HNO_3 prior to column chemistry. The chemical separation of K from other matrix elements followed the protocol outlined by Strelow et al. (1970) using Bio-Rad AG50W-X8 (200–400 mesh, H^+ form) cation exchange resin in 0.5 N HNO_3 eluent. The resin was cleaned alternately with Trace Metal grade (Fisher Scientific) 6 N HCl and water for three times and then double-distilled 1 N HNO_3 and water. Disposable Bio-Rad Poly-Prep

Table 1
Instrument operating parameters used in this study compared to previous studies using MC-ICPMS.

	This study	Morgan et al. (2018)	Li et al. (2016)	Wang and Jacobsen (2016)	Richter et al. (2011)
Instrument	Nu Plasma II Double-focusing	Neptune Plus Double-focusing	IsoProbe P Single-focusing with collision cell (He + H_2/D_2)	IsoProbe P Single-focusing with collision cell (H_2 + Ar)	IsoProbe P Single-focusing with collision cell (Ne + H_2)
Mass resolution	High resolution (~10,100)	High resolution (~10,000)	Low resolution (~400)	Low resolution (~400)	Low resolution (~400)
RF power	700–1125 W	500–600 W	1350 W	1350 W	1350 W
Introduction system	Dry plasma DSN-100 with 50–100 μL/min glass nebulizer	Wet plasma glass spray chamber with APEX PFA nebulizer	Wet plasma glass spray chamber with 100 μL/min glass nebulizer	Dry plasma Apex IR + ACM with 100 μL/min PFA nebulizer	Dry plasma Aridus II with 60 μL/min PFA nebulizer
Membrane gas flow	1.80–3.54 L/min	N/A	N/A	N/A	Unspecified
Hot gas flow	0.19–0.30L/min				
Nebulizer gas flow	15.6–39.8 psi	0.95–1.40 L/min	0.8–1.2 L/min	0.9 L/min	Unspecified
Cooling gas flow	13 L/min	18 L/min	13.1 L/min	13 L/min	Unspecified
Auxiliary gas flow	0.8–1.0 L/min	0.6–0.7 L/min	0.8–1.2 L/min	1.1 L/min	Unspecified
Data acquisition (integration time × cycle × block)	5 s × 50 × 1 = 250 s	8.389 s × 25 or 2.097 s × 80 = 168 s – 210 s	5 s × 40 × 1 = 200 s	10s × 30 × 1 = 300 s	5 s × 20 × 1 = 100 s

Table 2
Comparison of K isotopic compositions of various NIST SRM standards relative to NIST SRM 3141a.

Reference materials	Unit size	Primary usage	K concentration	Other main components	Homogeneity	Purity	$\delta^{41}K$ (‰)	2SD (‰)	95% c.i. (‰)	N
SRM 3141a (prepared from SRM 999a)	5 × 10 mL	standard for K element	10.003 ± 0.018 mg/g		Aqueous solution					
SRM 999c (KCl)	30 g	standard for K and Cl	52.443 ± 0.010 wt%	47.5519 ± 0.0081 wt% Cl	≥ 200 mg	99.987 ± 0.021 wt%	−0.01	0.09	0.02	22
							0.00	0.05	0.01	26
Wtd average							***0.00***	***0.04***		
SRM 918b (KCl)	30 g	standard for K and Cl	52.4121 ± 0.0086 wt%	47.5284 ± 0.0049 wt% Cl	≥ 250 mg	99.927 ± 0.014 wt%	0.07	0.06	0.01	26
							0.07	0.06	0.01	27
							0.08	0.05	0.05	5
							0.08	0.06	0.02	17
Wtd average							***0.08***	***0.03***		
SRM 193 (KNO_3)	90 g	standard for K in fertilizer	38.66 ± 0.01 wt%	13.85 wt% N	Unspecified	99.96 ± 0.02 wt%	0.02	0.05	0.01	16
							0.02	0.06	0.01	26
Wtd average							***0.02***	***0.04***		

For this and the following table, uncertainties are reported as both 2SD (two standard deviation) of repeated sample analyses and 95% confidence interval, i.e., 95% c.i. The 95% c.i. was corrected with Student *t*-factor (Platzner, 1997) and calculated based on 2SD of the bracketing standard in a session except when there was only one sample analyzed during a session, in which case the 2SD of sample measurements were used. N in this and the following table represents the number of analyses. The sample size required for homogeneity is provided in specific NIST certificates of analyses. The bold and italics in this and the following tables represent weighted (Wtd) averages calculated using Isoplot 3.75–4.15.

polyethylene columns were cleaned with repeated sequence of 10 mL water, 10 mL double-distilled 6 N HNO_3, and 10 mL water, and then filled with 2 mL of pre-cleaned resin (resin bed length 2.0 cm, diameter 0.8 cm). The resin was conditioned with 10 mL of 0.5 N HNO_3 before being loaded with 1 mL of sample solution. Matrix elements were eluted with 13 mL of 0.5 N HNO_3 and K was subsequently collected by passing 22 mL of 0.5 N HNO_3. Afterward, the K solutions were dried down and the purification process was repeated to ensure complete matrix removal.

2.3. Mass spectrometry

Potassium isotopic ratios were measured on a Nu Plasma II MC-ICPMS. Argon is the main plasma gas and it produces an intense background of $^{40}Ar^+$ on $^{40}K^+$, as well as direct isobaric interferences of $^{38}Ar^1H^+$ on $^{39}K^+$ and $^{40}Ar^1H^+$ on $^{41}K^+$. The $^{39}K^+$, $^{40}Ar^+$, and $^{41}K^+$ ion beams were simultaneously directed to Faraday cups L4, Ax, and H4, respectively. The Ax cup was blocked by a movable mask attached to the collector array; hence, only $^{39}K^+$ and $^{41}K^+$ were measured. The $^{38}Ar^1H^+$ interference on $^{39}K^+$ was found to be negligible due to the low natural abundance of $^{38}Ar^+$ versus $^{39}K^+$ (0.0632% vs. 93.2581%). By contrast, $^{40}Ar^1H^+$ presented a severe interference on $^{41}K^+$ and required a resolving power of ~4887 (10% valley definition) to distinguish, resulting in a narrow peak shoulder for $^{41}K^+$ in the analysis (Fig. 1a).

The following procedures were used to reduce the argon hydrides. First, RF forward power was lowered step-wise by 25 W from the normal setting of 1300 W. Similarly, the membrane gas flow rate of the DSN-100 desolvation nebulizer system was adjusted at each step to decrease the $^{40}Ar^1H^+/^{41}K^+$ ratio. The instrument was re-tuned after each step to maximize the beam stability and intensities of the K signals while minimizing isobaric interference. Second, a 30-μm source defining slit was used to achieve pseudo-high resolution mode. The slit clips the interfering $^{40}Ar^1H^+$ beam on the low mass side. Thus, measurements were carried out on the interference-free shoulders of $^{41}K^+$ and $^{39}K^+$ (Fig. 1b). Third, the width of the alpha slit, located before the ESA, was decreased to further reduce beam aberrations and sharpen the image. Fourth, "dry" plasma sample introduction was employed by using the DSN-100 fitted with a PFA spray chamber and a MicroMist glass nebulizer; this was used to increase sensitivity and reduce argide formation by removing the nitric acid solvent, i.e. N, O, and particularly H, were removed (Jakubowski et al., 1992). Typical instrumental parameters used here are reported in Table 1, along with those employed by other groups using MC-ICPMS.

Instrumental mass bias was corrected using sample-standard bracketing; each sample is referenced to the average of the two standard values that are measured before and after the sample measurement (Albarède and Beard, 2004). Each analysis represents an average of 50 cycles of 5 s on-peak integrations. A blank was measured at the beginning of an analytical session and was subtracted from the measured ion beams. The K isotopic composition is expressed in delta (δ) notation by following previous recommendation (Teng et al., 2017):

$$\delta^{41}K\ (‰) = \left\{ \frac{(^{41}K/^{39}K)_{sample}}{(^{41}K/^{39}K)_{standard}} - 1 \right\} \times 1000$$

The sample-standard sequence was repeated N times (N ≥ 4) to reduce instrumental-related random error and achieve better reproducibility. The reported isotopic composition for a given sample is the average of the N repeat analyses. Uncertainties are reported as both 2SD (two standard deviation of N repeated sample analyses during an analytical session) and 95% confidence interval (c.i.) calculated from standard error of the mean along with correction by Student *t*-factor ($\pm t \frac{SD}{\sqrt{N}}$, Platzner, 1997). For calculating the 95% c.i., when only one sample was measured, the standard deviation was calculated from the repeated measurements of the sample ($\delta^{41}K_{sample}$). For sessions that have more than one sample been measured, which were typically the case, there were considerably more analyses for bracketing standards than for individual samples. Thus the reproducibility of measured bracketing standards provides a better estimate of instrumental stability. For these samples, the standard deviation used in calculating the 95% c.i. was determined from the dispersion of $\delta^{41}K_{standard}$, which is the $\delta^{41}K$ value of the standard bracketed by the other two standards measured before and after.

3. Reference material for K isotopic analysis

One of the major obstacles in the emerging K isotope community is the lack of a universally accepted international reference material

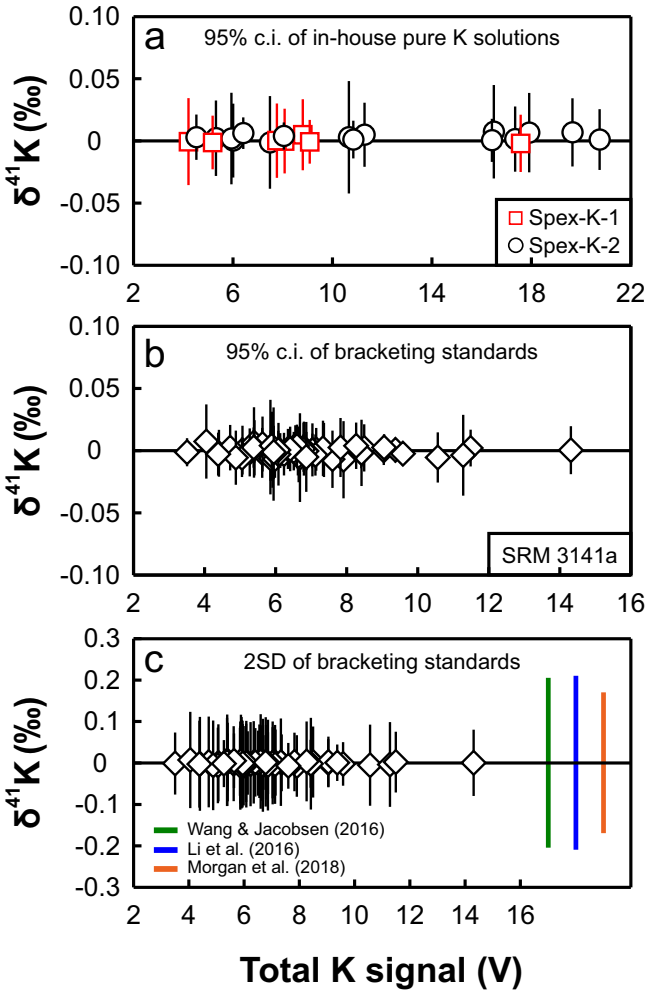

Fig. 2. Evaluation of external precision by multiple analyses on two in-house Spex K solutions (a) and the dispersion of bracketing standard NIST SRM3141a during different analytical sessions (b and c) over a six-month period. Results are plotted as a function of total K beam intensities (V). Typical external precision (2SD) reported in other laboratories were plotted in (c) for comparison. The 2SD plotted from Wang and Jacobsen (2016) is the average of their 2SD values.

against which to report K isotopic data, making direct inter-laboratory comparison difficult. The few published high-precision K isotope data by MC-ICPMS were reported relative to several different reference materials. For example, Wang and Jacobsen (2016) recommended to use Bulk Silicate Earth (BSE) while Morgan et al. (2018) suggested seawater, and Li et al. (2016) used a purified KNO_3 solution (SRM 3141a) from National Institute of Standards and Technology (NIST). A few recent studies on boninites, pegmatites, and sedimentary rocks have found up to 1.82‰ variation in $\delta^{41}K$ (Parendo et al., 2017; Morgan et al., 2018), suggesting that the BSE may not be a homogeneous K isotopic baseline at the high precisions that are now achievable. Here, we investigated the K isotopic compositions of four currently available certified reference materials from NIST, including SRM 193, SRM 918b, SRM 999c, and SRM 3141a, to assess which one has a $\delta^{41}K$ value that is closest to terrestrial values, and hence will be the most suitable standard for K isotopic analysis. The results suggest that all the four NIST elemental K standards are isotopically lighter than seawater (Table 2). Furthermore, SRM 193 and 999c have similar K isotopic ratios to that of the solution standard SRM 3141a, whereas SRM 918b has a slightly heavier $\delta^{41}K$ than SRM 3141a. As a result, SRM 193, 999c and 3141a are the preferred reference materials since the K isotopic values measured against any of them could be compared

Table 3
K isotopic compositions of pure K solution standards measured (relative to themselves) in this study.

Sample	$\delta^{41}K$ (‰)	2SD (‰)	95% c.i. (‰)	N
Spex-K-1	0.00	0.07	0.02	11
	0.00	0.10	0.03	13
	0.00	0.10	0.04	10
	0.00	0.11	0.02	28
	0.00	0.09	0.03	14
	0.00	0.11	0.02	37
	0.00	0.08	0.03	10
Wtd average	***0.00***	***0.03***		
Spex-K-2	0.00	0.10	0.02	47
	0.00	0.08	0.03	12
	0.00	0.11	0.03	20
	0.00	0.10	0.02	36
	0.00	0.07	0.01	43
	0.00	0.08	0.02	22
	0.00	0.11	0.03	15
	0.00	0.11	0.03	15
	0.01	0.05	0.03	6
	0.01	0.11	0.04	11
	0.01	0.11	0.03	14
	0.00	0.08	0.02	13
	0.00	0.10	0.04	10
	0.01	0.09	0.01	50
	0.00	0.08	0.04	7
	0.00	0.11	0.05	8
Wtd average	***0.00***	***0.02***		
SRM 3141a	0.00	0.08	0.02	23
	0.00	0.09	0.02	18
	−0.01	0.10	0.02	25
	0.00	0.07	0.01	26
	0.00	0.08	0.02	19
	0.00	0.07	0.02	12
	0.00	0.08	0.04	7
	0.00	0.09	0.02	23
	0.00	0.07	0.01	33
	0.00	0.09	0.02	22
	−0.01	0.11	0.04	12
	0.00	0.08	0.01	31
	0.00	0.06	0.01	25
	0.00	0.09	0.02	22
	0.00	0.06	0.01	27
	0.00	0.04	0.01	25
	0.00	0.06	0.01	34
	0.00	0.05	0.01	35
	0.00	0.09	0.02	31
	0.00	0.07	0.01	45
	0.00	0.09	0.02	24
	0.00	0.11	0.03	15
	0.00	0.10	0.04	10
	0.00	0.10	0.03	12
	0.00	0.09	0.02	24
	0.01	0.11	0.03	17
	−0.01	0.07	0.03	8
	−0.01	0.06	0.02	8
	0.00	0.06	0.02	11
	0.00	0.10	0.01	55
	0.00	0.09	0.02	19
	−0.01	0.11	0.02	37
	0.01	0.07	0.02	11
	0.00	0.06	0.02	10
	0.00	0.11	0.02	37
	0.00	0.11	0.02	37
	−0.01	0.10	0.02	41
	0.00	0.10	0.02	36
	0.00	0.11	0.03	19
	0.00	0.11	0.02	24
	0.00	0.09	0.02	20
	0.01	0.12	0.03	17
	−0.01	0.09	0.02	36
	−0.01	0.11	0.02	26
	0.00	0.07	0.02	11
	0.00	0.10	0.02	39
	0.00	0.11	0.02	31
	0.00	0.10	0.02	34

(*continued on next page*)

Table 3 (*continued*)

Sample	δ^{41}K (‰)	2SD (‰)	95% c.i. (‰)	N
	0.00	0.07	0.02	25
	0.00	0.08	0.02	27
	0.00	0.07	0.01	39
	0.00	0.10	0.02	39
	0.00	0.10	0.02	28
	0.00	0.11	0.02	44
	0.00	0.11	0.03	19
	0.00	0.11	0.02	45
	0.00	0.08	0.02	23
	0.00	0.10	0.03	19
	0.00	0.09	0.02	38
	0.00	0.10	0.02	21
	0.00	0.11	0.02	38
	−0.01	0.11	0.03	17
Wtd average	***0.00***	***0.01***		

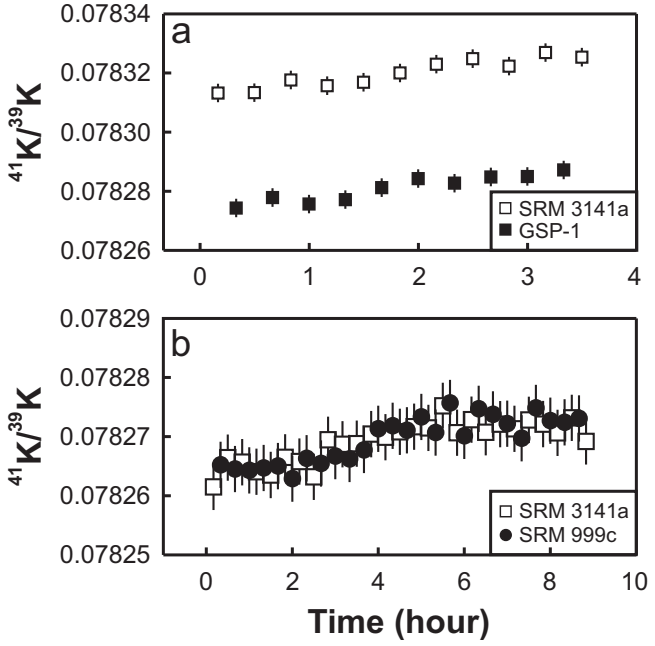

Fig. 3. Examples of repeat measurements on a UGSG rock standard GSP-1 (a), and a NIST SRM 999c K standard (b) showing short-term reproducibility and drift in instrumental mass bias with time. Error bars are 2SD of multiple sample measurements (0.04‰ and 0.05‰ for a and b, respectively).

directly, and their K isotopic compositions fall in the range of natural samples.

Following the practice of Li et al. (2016), we suggest the community to adopt SRM 3141a as the reference material for reporting K isotopic data in the future because it meets the requirements for a reference material best (see summary in Teng et al., 2017). Firstly, SRM 3141a is a high purity 10,000 mg/kg K solution with a long shelf life that can be used directly without the potential uncertainty caused by digestion and column purification, as well as intrinsic solid standard heterogeneity, which is more pertinent as analytical precision improves. For example, standards SRM 999c and 918b require a sample size larger than 200 mg and 250 mg, respectively, to obtain a homogeneous solution, as instructed by NIST's certificates of analysis (Table 2). Secondly, SRM 3141a is readily accessible from NIST, in contrast to some in-house standards that have much more restricted availability. Thirdly, this standard has a δ^{41}K value falling between modern seawater and typical crustal rocks, two major K reservoirs. Finally, SRM 3141a is prepared from SRM 999a and previous data reported by Morgan et al. (2018), which were measured relative to SRM 999b, can be directly compared with those reported by Li et al. (2016) and this study.

Table 4
K isotopic compositions of natural standards measured (relative to SRM 3141a) in this study.

Sample	δ^{41}K (‰)	2SD (‰)	95% c.i. (‰)	N
Hawaiian seawater	0.14	0.06	0.04	5
	0.14	0.05	0.04	6
Wtd average	***0.14***	***0.04***		
BHVO-1	−0.43	0.06	0.05	5
Duplicate	−0.42	0.02	0.05	4
Wtd average	***−0.42***	***0.02***		
BCR-1	−0.42	0.06	0.03	8
AGV-1	−0.45	0.05	0.02	12
GSP-1	−0.50	0.04	0.02	10
G-2	−0.45	0.05	0.04	6
Replicate	−0.46	0.05	0.03	6
Wtd average	***−0.46***	***0.04***		
SGR-1	−0.25	0.05	0.05	5
Duplicate	−0.25	0.05	0.04	6
Wtd average	***−0.25***	***0.04***		

Duplicate represents repeat analyses on the same purified sample during different sessions. Replicate represents repeat sample dissolution, column chemistry, and instrumental analyses.

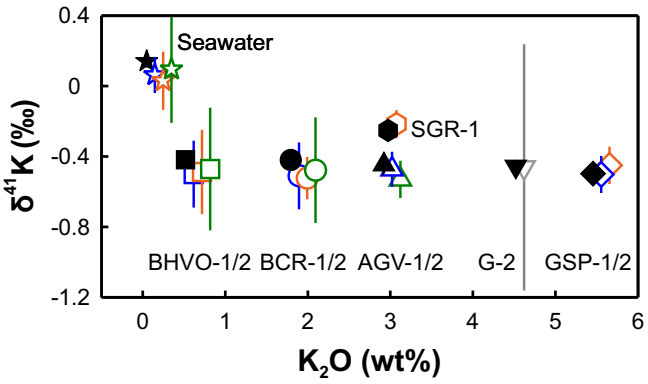

Fig. 4. Inter-laboratory comparison of natural standard δ^{41}K data measured in this study (black solid symbols) with those reported by other laboratories (colored open symbols). The grey, blue, green, and orange symbols represent data from Humayun and Clayton (1995b), Li et al. (2016), Wang and Jacobsen (2016), and Morgan et al. (2018), respectively. All data on this figure are normalized to NIST SRM 3141a with 2SD error bars. When not seen, the error bars are smaller than the symbols. The K_2O contents for USGS standards are from their corresponding certificates of analyses (recalculated to volatile-free compositions), and that of seawater is from Li and Schoonmaker (2014). (For interpretation of the references to colour in this figure legend, the reader is referred to the web version of this article.)

4. Precision and accuracy

Precision and accuracy of our analytical procedure were evaluated by repeated analyses of several pure K standard solutions from Spex CertiPrep and NIST, as well as natural samples including Hawaiian seawater and six USGS rock standards.

The within-run precision of the ^{41}K/^{39}K ratio for a single measurement consisting of one block of 50-ratio analyses was typically between 0.02 and 0.03‰ (2SD). The external precision (95% c.i.) was evaluated through multiple analyses of two in-house K solutions (Spex-K-1 and Spex-K-2), seven natural standards, as well as the dispersion of bracketing standards (NIST SRM 3141a) during different analytical sessions over a six-month period (2017 November to 2018 April). Results of duplicate (repeat analyses on a same purified K solution) and replicate (repeat sample dissolution, column chemistry, and instrumental analyses) on synthetic and natural standards were both reproducible within

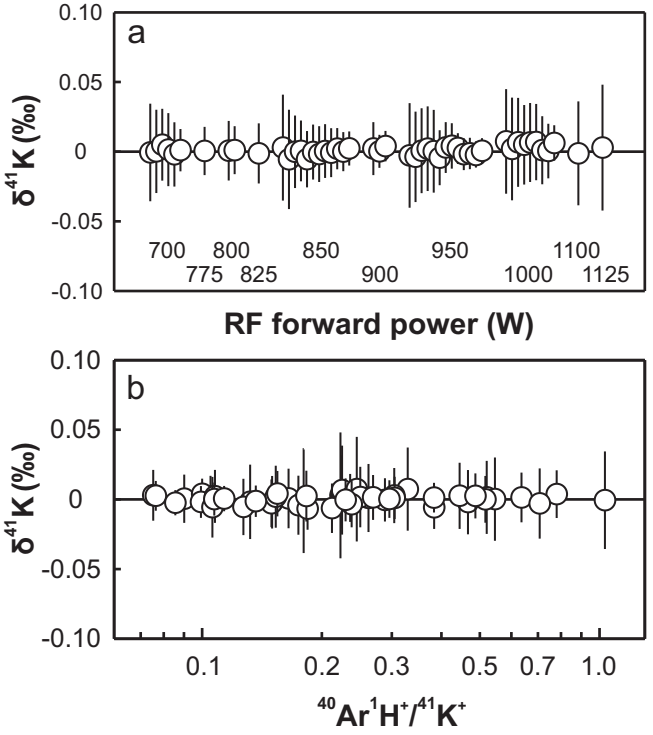

Fig. 5. Multiple analyses on pure K solutions as a function of RF forward power (a) and $^{40}Ar^{1}H^{+}/^{41}K^{+}$ ratio (b). Error bars in this and following figures are Student *t* factor-corrected 95% c.i. unless specified otherwise.

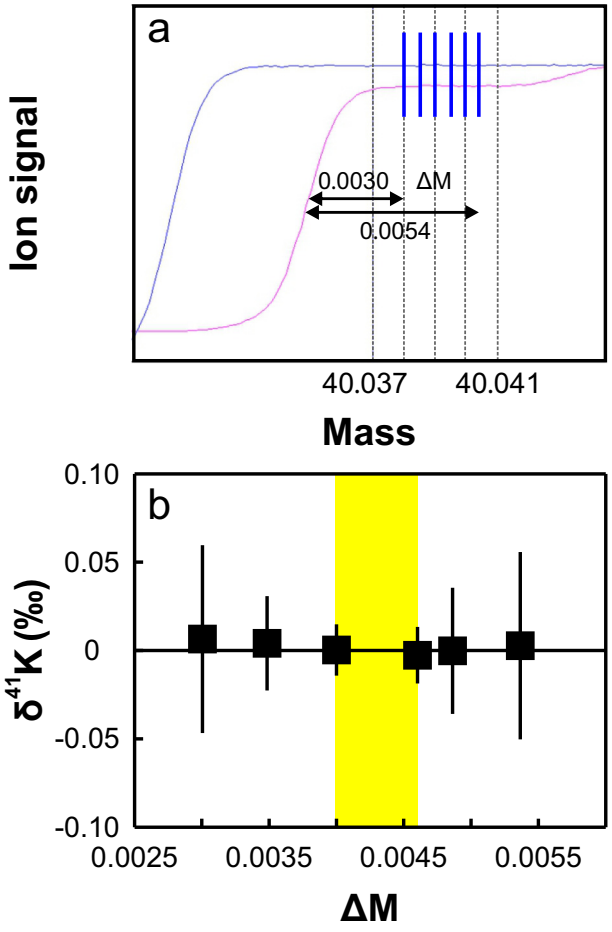

Fig. 6. Test of peak flatness and interference tailing on K isotope measurement. The yellow area in the figure represents the ΔM range used in the rest of the measurements in this study. Refer to Fig. 1b for the definition of ΔM. (For interpretation of the references to colour in this figure legend, the reader is referred to the web version of this article.)

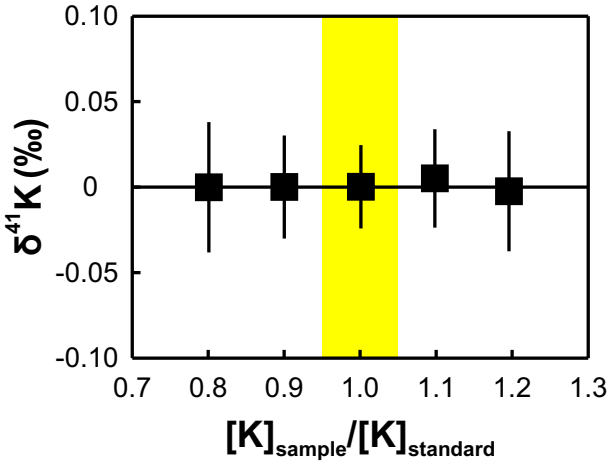

Fig. 7. Effects of K concentration mismatch between samples and bracketing standards. The K concentrations of sample and standard are always matched to within 5% (yellow area in the figure) for the rest of the measurements in this study. (For interpretation of the references to colour in this figure legend, the reader is referred to the web version of this article.)

0.01‰ (Tables 2 and 4). A total of 23 repeat measurements on two Spex CertiPrep KNO_3 solutions (two different bottles) bracketed by themselves yielded 95% c.i. varying from of 0.01‰ to 0.05‰ and 2SD from 0.07‰ to 0.11‰ (Fig. 2a; Table 3). The bracketing standard NIST 3141a yielded 95% c.i. ranging from 0.01‰ to 0.04‰ and 2SD from 0.04‰ to 0.11‰ during 62 individual analytical sessions (Fig. 2b,c; Table 3). Taking the range of 2SD from these K standard measurements (Fig. 2c) as a representative range of 2SD for the bracketing standards during an analytical session, the expected precision (95% c.i.) for a sample that is typically measured for ≥4 times would be < 0.06‰. Based on these results, the external precision of our analytical routine is conservatively estimated to be better than 0.06‰ (95% c.i.), which is calculated from the 2SD of bracketing standard during a full analytical session and is further corrected by Student *t*-factor. The routine precision by our analytical protocol is similar to, or better than, those reported recently by other laboratories based on two standard error (2SE) calculated from 2SD of repeat sample measurements without Student-*t* correction (0.05‰ to 0.07‰, Li et al., 2016; Wang and Jacobsen, 2016; Morgan et al., 2018). Our quoted external precision (95% c.i. < 0.06‰) is also comparable to the 2SD of multiple sample measurements, which typically falls in the range of 0.02‰ to 0.06‰ (Fig. 3, Table 4). It is noteworthy that the 2SD of repeated sample analyses obtained in our laboratory is significantly smaller than those reported by other laboratories (~0.2‰) with similar numbers of repeated analyses (N = 4 to 10) (Li et al., 2016; Wang and Jacobsen, 2016; Morgan et al., 2018).

The accuracy of our analytical protocol is assessed by measurements on both pure K standards and chemically-purified natural samples (Tables 2–4). Three pure K solutions bracketed by themselves yielded $\delta^{41}K$ values between −0.01‰ and 0.01‰, agreeing to the expected value of 0 within uncertainties (Fig. 2). Analyses on SRM 918b ($\delta^{41}K_{SRM3141a} = 0.08 \pm 0.03$‰, 2SD) and SRM 999c ($\delta^{41}K_{SRM3141a} = 0.00 \pm 0.04$‰, 2SD) against SRM 3141a also yielded results that are consistent with those reported by Morgan et al. (2018)

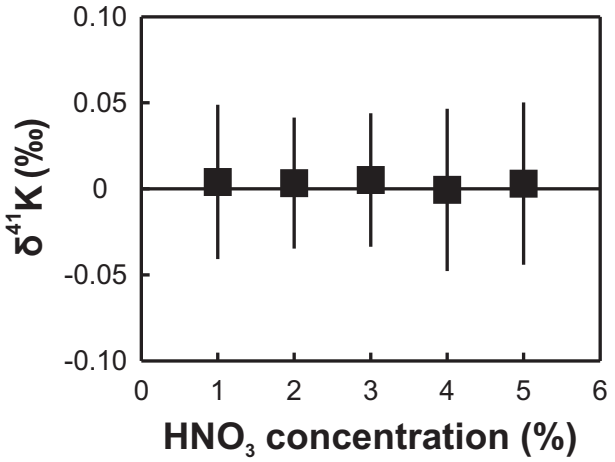

Fig. 8. Effects of HNO_3 concentration (v/v) mismatch between samples and bracketing standards.

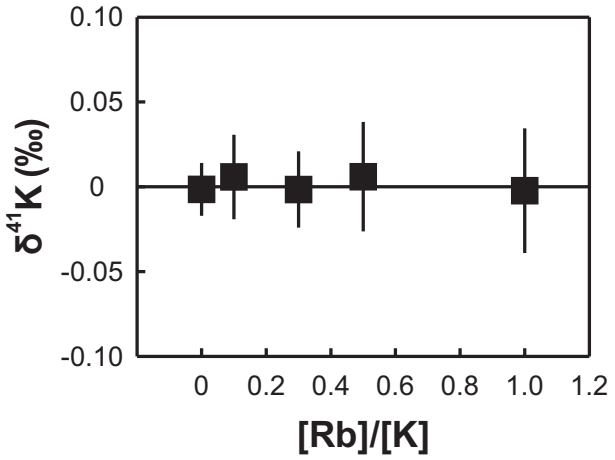

Fig. 9. Effects of presence of the matrix element Rb on K isotope analysis.

(SRM 918 = 0.00 ± 0.22‰, 2SD and SRM 999b = 0.00 ± 0.17‰, 2SD). Additionally, the identical isotopic ratios obtained for SRM 999c and SRM 3141a further substantiate the accuracy of our method since SRM 3141a was prepared from SRM 999a.

The whole-procedure accuracy of our analytical routine is validated by consistent results obtained between our and other laboratories for seven chemically-processed natural sample standards with different elemental matrices (Fig. 4). Five USGS igneous rock standards varying in composition from basalt to granite, yet fall in a narrow range of $\delta^{41}K$, from −0.50 ± 0.04‰ (2SD, N = 10) to −0.42 ± 0.02‰ (2SD, N = 9), in agreement with previously published data (Humayun and Clayton, 1995b; Wang and Jacobsen, 2016; Li et al., 2016; Morgan et al., 2018). The petroleum and carbonate-rich shale (SGR-1) has a comparatively higher $\delta^{41}K$ of −0.25 ± 0.04‰ (2SD, N = 11), consistent with the value reported by Morgan et al. (2018). In contrast to rock samples, the seawater sample from Hawaii is characterized by a high $\delta^{41}K$ of 0.14 ± 0.04‰ (2SD, N = 11), similar to reported seawater values from various locations (Wang and Jacobsen, 2016; Li et al., 2016; Morgan et al., 2018). The resolvable terrestrial K isotopic variations between different types of rocks and between rocks and seawater suggest the potential application of K isotope systematics as a new tracer for processes such as low-temperature water-rock interactions, which in turn emphasizes the importance of acquiring high-precision and high-accuracy $\delta^{41}K$ data. The following section provides a detailed examination on how to achieve high-precision K isotopic data through optimization of various parameters.

5. Optimization of K isotopic analysis

The acquisition of precise and accurate K isotopic data by MC-ICPMS can be affected by a number of factors, the most important of which include the amount of argon hydrides, the flatness of the peak shoulder, K concentration, acid strength, and presence of matrix elements. Below we examine these factors in turn to propose a robust and optimized protocol for routine high-precision measurements of K isotope ratios.

5.1. RF forward power

The major analytical difficulty intrinsic to K isotope measurements by MC-ICPMS is the interference from argon hydrides, particularly $^{40}Ar^{1}H^{+}$, which results in a tailing effect on $^{41}K^{+}$. Operating the plasma under lower power has been shown to significantly suppress the formation of argon hydrides as the dominant polyatomic backgrounds changed from Ar-related species to NO^{+} (Jiang et al., 1988). Therefore, RF has been reduced from full power of 1300 W along with re-tuning of the DSN-100 membrane gas flow rate, until no significant further decrease in $^{40}Ar^{1}H^{+}/^{41}K^{+}$ ratio was observed. The optimal RF power varies between analytical sessions, but a range of 700 W to 1125 W was found to be able to effectively lower the $^{40}Ar^{1}H^{+}/^{41}K^{+}$ ratios to below one, which are sufficient for achieving a precision of better than 0.06‰ (95% c.i.) (Fig. 5).

5.2. Peak shoulder flatness

Isotopic measurements using pseudo-high resolution is particularly prone to the tailing effect; therefore, a flat peak shoulder is essential for achieving high-precision measurements. Given the narrow width of the resolved $^{41}K^{+}$ shoulder, analytical accuracy and precision are sensitive to the selected analysis mass position (Fig. 6). The width of the flat $^{41}K^{+}$ shoulder has been tested by measuring K isotopic ratios at different positions on the peak shoulder. The results suggest that although all the measured $\delta^{41}K$ values are close to zero, uncertainties increase noticeably as the analyses were carried out further away from the center of the peak shoulder (Fig. 6). Consequently, all the measurements in this study were performed using a ΔM value between 0.0040 and 0.0046 amu, corresponding to a flat shoulder width of approximately 100 ppm, about double width achieved by Morgan et al. (2014) on a Neptune Plus MC-ICPMS (~50 ppm).

5.3. K concentration mismatch between samples and bracketing standards

Instrumental mass bias for K isotopic analysis by MC-ICPMS is large (~8%) and drifts with time (Fig. 3). Therefore, sample-standard bracketing method was used by assuming instrumental mass bias for sample and standard is the same. This requires that the sample and standard have identical K concentrations. However, dilution processes before a batch run could lead to different K concentrations between and among samples and bracketing standards, which we refer to as a concentration mismatch. This effect on K isotopic analysis was evaluated by bracketing measurements of the same pure K standards but with deliberately mismatched K concentrations. The results suggest that K concentration mismatch does not result in significant deviation if the sample and standard concentrations match to within 20% (Fig. 7). Nevertheless, K concentrations in samples and standards were matched to within 5% for all other measurements conducted in this study.

5.4. Acid molarity mismatch between samples and bracketing standards

Sample solutions are typically introduced into the MC-ICPMS in dilute acids. Mismatch in acid molarity between sample and bracketing standard could cause variations in space charge effects and hence instrumental mass bias, leading to analytical artifacts, as have been

observed for Mg and Fe isotope measurements (Dauphas et al., 2009; Teng and Yang, 2014). This possibility on K isotopic analysis was tested by measuring pure K solutions in 1% to 5% HNO_3 (v/v) against that in 3% HNO_3 (v/v). The results reveal no measurable influence of acid strength on K isotopic data quality (Fig. 8). Nevertheless, since subtraction of on-peak-zero (OPZ) ion intensities was used in this study, sample and standard in the rest of the measurements were diluted to the same K concentration to within 5% using the same batch of 3% HNO_3. While this is easily achievable for MC-ICPMS analyses, it also ensures that all the sample and standard solutions are in the same medium and thus have the same acid-induced background. As such, only one OPZ measurement per session is sufficient.

5.5. Matrix effects

Presence of matrix elements is another critical factor that could change the instrumental mass bias encountered by the sample and bracketing standard, violating the prerequisite for applying sample-standard bracketing. In contrast to the bracketing standard that is typically a pure element solution, natural samples have a large variation in [matrix elements]/[K] concentration ratio. Although column chemistry can separate K from most of the matrix elements, there remains the possibility that some matrix elements may be retained in purified K solutions. Since cold plasma condition enhances the formation of matrix-induced polyatomic species (Murphy et al., 2002), whether or not the presence of matrix elements will bias the measured $\delta^{41}K$ values needs to be investigated.

The effects of Mg, Ca and Na impurities are of primary consideration since they form polyatomic species that are isobaric to K isotopes ($^{23}Na^{16}O^+$ on $^{39}K^+$, $^{25}Mg^{16}O^+$, $^{23}Na^{18}O^+$ and $^{40}Ca^1H^+$ on $^{41}K^+$). Morgan et al. (2018) examined the influences from Ca and Mg and concluded that these impurities will not cause significant interference until they reach 20–30% of the K concentrations. Seawater has a much higher [Na]/[K] ratio (~46, Li and Schoonmaker, 2014) than typical rocks. The consistent $\delta^{41}K$ values of seawater obtained from our and other laboratories (Fig. 4) suggest that Na is not an issue in column separation. For our column chemistry protocol, the only element that cannot be quantitatively removed from K is rubidium (Rb), as these two elements have similar relative selectivity for Bio-Rad AG 50W-X8 cation exchange resin (Strelow et al., 1970). We thereby tested the influence of Rb on K isotope analysis by deliberately doping the pure K solutions with Rb in a range of [Rb]/[K] concentration ratio from 0.1 to 1.0. These Rb-doped K solutions were then measured against pure K solutions. The results suggest that the presence of Rb with [Rb]/[K] concentration ratio up to one does not affect measured $\delta^{41}K$ values within our analytical uncertainties (Fig. 9). Since natural samples generally have [Rb]/[K] ratios much lower than one, these results also support the accuracy of our column chemistry.

6. Conclusions

This study presents an optimized protocol for high accuracy and precision (better than 0.06‰, 95% c. i.) measurements of K isotope ratios in both rock and water samples using a Nu Plasma II MC-ICPMS. Formation of argon hydrides is suppressed by using reduced RF forward power and “dry” plasma sample introduction via a DSN-100 desolvation system while the interference of $^{40}Ar^1H^+$ on $^{41}K^+$ is resolved by high mass resolution. By lowering the RF power to the range of 700 W to 1125 W, the $^{40}Ar^1H^+/^{41}K^+$ ratio can be reduced to below one, sufficiently low for high-precision K isotopic analysis. Partial separation of $^{40}Ar^1H^+$ from $^{41}K^+$ results in a flat peak shoulder of ~100 ppm width, wide enough to neglect the effect of magnet drift during an analytical session. Although mismatches in K concentration and acid molarity between samples and bracketing standards do not result in a measurable effect on $\delta^{41}K$, matching them to within 5% is recommended to avoid potential analytical artifacts. Analyses of seawater and USGS rock standards with various compositions revealed a large K isotopic variation, and K isotopes may thus be a promising tracer for water-rock interactions and crustal recycling.

Acknowledgements

We would like to thank Yang Sun and Tian-Yi Huang for assistance with laboratory work. Bruce Nelson, Ronald Sletten, and Scott Kuehner are acknowledged for their suggestions to improve this study. Constructive comments from Paul Tomascak and an anonymous reviewer, and efficient editorial handling by Catherine Chauvel are gratefully acknowledged.

References

Albarède, F., Beard, B.L., 2004. Analytical methods for non-traditional isotopes. Rev. Mineral. Geochem. 55, 113–151.
Alexander, C.M.O'.D., Grossman, J.N., 2005. Alkali elemental and potassium isotopic compositions of Semarkona chondrules. Meteorit. Planet. Sci. 40, 541–556.
Alexander, C.M.O'.D., Grossman, J.N., Wang, J., Zanda, B., Bourot-Denise, M., Hewins, R.H., 2000. The lack of potassium isotopic fractionation in Bishunpur chondrules. Meteorit. Planet. Sci. 35, 859–868.
Arevalo, R., 2016. Potassium. In: White, W.M. (Ed.), Encyclopedia of Geochemistry. Springer. http://dx.doi.org/10.1007/978-3-319-39193-9_132-1.
Barnes, I.L., Garner, E.L., Gramlich, J.W., Machlan, L.A., Moody, J.R., Moore, L.J., Murphy, T.J., Shields, W.R., 1973. Isotopic abundance ratios and concentrations of selected elements in some Apollo 15 and Apollo 16 samples. In: Proc. 2nd Lunar Sci. Conf. pp. 1197–1207.
Becker, J.S., Dietze, H.-J., 1998. Ultratrace and precise isotope analysis by double-focusing sector field inductively coupled plasma mass spectrometry. J. Anal. At. Spectrom. 13, 1057–1063.
Becker, J.S., Füllner, K., Seeling, U.D., Fornalczyk, G., Kuhn, A.J., 2008. Measuring magnesium, calcium and potassium isotope ratios using ICP-QMS with an octopole collision cell in tracer studies of nutrient uptake and translocation in plants. Anal. Bioanal. Chem. 390, 571–578.
Berglund, M., Wieser, M.E., 2011. Isotopic compositions of the elements 2009 (IUPAC Technical Report). Pure Appl. Chem. 83, 397–410.
Brewer, A.K., 1936. The abundance ratio of the isotopes of potassium in mineral and plant sources. J. Am. Chem. Soc. 58, 365–370.
Brewer, A.K., 1937. Abundance ratio of the isotopes of potassium in animal tissues. J. Am. Chem. Soc. 59, 869–872.
Church, S.E., Tilton, G.R., Wright, J.E., Lee-Hu, C.-N., 1976. Volatile element depletion and $^{39}K/^{41}K$ fractionation in lunar soils. In: Proc. Lunar Sci. Conf. 7th, Geochim. Cosmochim. Acta Suppl. vol. 7. pp. 423–439.
Dauphas, N., Pourmand, A., Teng, F.-Z., 2009. Routine isotopic analysis of iron by HR-MC-ICPMS: how precise and how accurate? Chem. Geol. 267, 175–184.
Garner, E.L., Machlan, L.A., Barnes, I.L., 1975. The isotopic composition of lithium, potassium, and rubidium in some Apollo 11, 12, 14, 15, and 16 samples. In: Proc. 6th Lunar Sci. Conf. pp. 1845–1855.
Gramlich, J.W., Machlan, L.A., Brletic, K.A., Kelly, W.R., 1982. Thermal-ionization isotope-dilution mass spectrometry as a definitive method for determination of potassium in serum. Clin. Chem. 28, 1309–1313.
Humayun, M., Clayton, R.N., 1995a. Potassium isotope cosmochemistry – genetic-implications of volatile element depletion. Geochim. Cosmochim. Acta 59, 2131–2148.
Humayun, M., Clayton, R.N., 1995b. Precise determination of the isotopic composition of potassium: application to terrestrial rocks and lunar soils. Geochim. Cosmochim. Acta 59, 2115–2130.
Humayun, M., Koeberl, C., 2004. Potassium isotopic composition of Australasian tektites. Meteorit. Planet. Sci. 39, 1509–1516.
Jakubowski, N., Feldmann, I., Stuewer, D., 1992. Analytical improvement of pneumatic nebulization in ICP-MS by desolvation. Spectrochim. Acta 47B, 107–118.
Jiang, S.J., Houk, R.S., Stevens, M.A., 1988. Alleviation of overlap interferences for determination of potassium isotope ratios by inductively coupled plasma mass spectrometry. Anal. Chem. 60, 1217–1221.
Li, Y.-H., Schoonmaker, J.E., 2014. Chemical composition and mineralogy of marine sediments. In: Treatise on Geochemistry. vol. 7. Elsevier Ltd, pp. 1–35.
Li, W., Beard, B.L., Li, S., 2016. Precise measurement of stable potassium isotope ratios using a single focusing collision cell multi-collector ICP-MS. J. Anal. At. Spectrom. 31, 1023–1029.
Midwood, A.J., Proe, M.F., Harthill, J.J., 2000. Use and analysis by thermal ionization mass spectrometry of Mg and K to assess mineral uptake in Scots pine (*Pinus sylvestris* L.). Analyst 125, 487–492.
Morgan, L.E., Higgins, J., Davidheiser-Kroll, B., Lloyd, N., Faithfull, J., Ellam, R., 2014. Potassium Isotope Geochemistry and Magmatic Processes. (Goldschmidt Conference abstract).
Morgan, L.E., Ramos, D.P.S., Davidheiser-Kroll, B., Faithfull, J., Lloyd, N.S., Ellam, R.M., Higgins, J.A., 2018. High-precision $^{41}K/^{39}K$ measurements by MC-ICP-MS indicate terrestrial variability of $\delta^{41}K$. J. Anal. At. Spectrom. http://dx.doi.org/10.1039/C7JA00257B.
Murphy, K.E., Long, S.E., Rearick, M.S., Ertas, Ö.S., 2002. The accurate determination of potassium and calcium using isotope dilution inductively coupled “cold” plasma mass

spectrometry. J. Anal. At. Spectrom. 17, 469–477.
Nier, A.O., 1936. A mass-spectrographic study of the isotopes of argon, potassium, rubidium, zinc and cadmium. Phys. Rev. 50, 1041–1045.
Nier, A.O., 1950. A redetermination of the relative abundances of the isotopes of carbon, nitrogen, oxygen, argon, and potassium. Phys. Rev. 77, 789–793.
Parendo, C.A., Yamashita, K., Jacobsen, S.B., Okano, O., 2017. Potassium isotope variations in forearc boninite-series volcanics from Chichijima. In: American Geophysical Union Fall Meeting, V13E-07.
Platzner, I.T., 1997. Modern Isotope Ratio Mass Spectrometry. John Wiley & Sons, Chichester (514 pp.).
Richter, F.M., Mendybaev, R.A., Christensen, J.N., Ebel, D., Gaffney, A., 2011. Laboratory experiments bearing on the origin and evolution of olivine-rich chondrules. Meteorit. Planet. Sci. 46, 1152–1178.
Richter, F.M., Bruce, Watson E., Chaussidon, M., Mendybaev, R., Christensen, J.N., Qiu, L., 2014. Isotope fractionation of Li and K in silicate liquids by Soret diffusion. Geochim. Cosmochim. Acta 138, 136–145.
Strelow, E.W.E., Von, S., Toerien, F., Weinert, C.H.S.W., 1970. Accurate determination of traces of sodium and potassium in rocks by ion exchange followed by atomic absorption spectroscopy. Anal. Chim. Acta 50, 399–405.
Taylor, T.I., Urey, H.C., 1938. Fractionation of the lithium and potassium isotopes by chemical exchange with zeolites. J. Chem. Phys. 6, 429–438.
Taylor, S., Delaney, J., Ma, P., Herzog, G.F., Engrand, C., 2005. Isotopic fractionation of iron, potassium, and oxygen in stony cosmic spherules: implications for heating histories and sources. Geochim. Cosmochim. Acta 69, 2647–2662.
Teng, F.-Z., Yang, W., 2014. Comparison of factors affecting the accuracy of high-precision magnesium isotope analysis by multi-collector inductively coupled plasma mass spectrometry. Rapid Commun. Mass Spectrom. 28, 19–24.
Teng, F.-Z., Dauphas, N., Watkins, J., 2017. Non-traditional stable isotopes: Retrospective and prospective. Rev. Mineral. Geochem. 82, 1–26.
Wang, K., Jacobsen, S.B., 2016. An estimate of the Bulk Silicate Earth potassium isotopic composition based on MC-ICPMS measurements of basalts. Geochim. Cosmochim. Acta 178, 223–232.
Yu, Y., Hewins, R.H., Alexander, C.M.O., Wang, J., 2003. Experimental study of evaporation and isotopic mass fractionation of potassium in silicate melts. Geochim. Cosmochim. Acta 67, 773–786.